The Journal of Neuroscience, August 1988, 8(8): 2913–2927

Primate Motor Cortex and Free Arm Movements to Visual Targets in Three-Dimensional Space. I. Relations Between Single Cell Discharge and Direction of Movement

Andrew B. Schwartz,[a] Ronald E. Kettner,[b] and Apostolos P. Georgopoulos

The Philip Bard Laboratories of Neurophysiology, Department of Neuroscience, The Johns Hopkins University, School of Medicine, Baltimore, Maryland 21205

We describe the relations between the neuronal activity in primate motor cortex and the direction of arm movement in three-dimensional (3-D) space. The electrical signs of discharge of 568 cells were recorded while monkeys made movements of equal amplitude from the same starting position to 8 visual targets in a reaction time task. The layout of the targets in 3-D space was such that the direction of the movement ranged over the whole 3-D directional continuum in approximately equal angular intervals. We found that the discharge rate of 475/568 (83.6%) cells varied in an orderly fashion with the direction of movement: discharge rate was highest with movements in a certain direction (the cell's "preferred direction") and decreased progressively with movements in other directions, as a function of the cosine of the angle formed by the direction of the movement and the cell's preferred direction. The preferred directions of different cells were distributed throughout 3-D space. These findings generalize to 3-D space previous results obtained in 2-D space (Georgopoulos et al., 1982) and suggest that the motor cortex is a nodal point in the construction of patterns of output signals specifying the direction of arm movement in extrapersonal space.

The cortical mechanisms controlling arm movements in two-dimensional (2-D) space have been the object of several recent studies (Georgopoulos et al., 1982, 1983, 1984, 1985; Kalaska et al., 1983, 1985; Georgopoulos and Massey, 1985). The variation in cell discharge was studied in relation to movement of the arm in extrapersonal space rather than to motion of the limb about a single joint. It was found that the frequency of discharge of single cortical cells is a relatively simple, broad tuning function of the direction of movement in space, in spite of the fact that the movements studied involved motion at 2 joints (the shoulder and the elbow) and were produced by complicated muscle synergies (Georgopoulos et al., 1984). This relation holds both for the motor cortex (Georgopoulos et al., 1982), which is linked to the control of muscles and movements, and for area 5 of the posterior parietal cortex (Kalaska et al., 1983), which is related mainly to afferent proprioceptive input (Duffy and Burchfiel, 1971; Sakata et al., 1973) but also to the control of movement (Mountcastle et al., 1975). The directional tuning is described by a cosine function, such that the frequency of discharge of a single cell is highest with movements in a particular, "preferred" direction, and decreases progressively with movements in other directions. Those results were obtained for movements that monkeys learned to make using an articulated manipulandum. Would that relation generalize to free arm movements in three-dimensional (3-D) space? We investigated this question by studying the activity of single cells in the motor cortex of monkeys trained to reach out in 3-D space to push lighted buttons. Preliminary results were described previously (Georgopoulos et al., 1986).

Materials and Methods

Apparatus. The apparatus used (Fig. 1*A*) allowed reaching to visual targets in 3-D space. It consisted of a metal plate placed in front of the animal and metal rods threaded through holes cut in the plate. The front end of each rod housed a red button 16 mm in diameter that could be lighted and, if depressed by a minimum force of approximately 200 gm, close a switch. Nine rods were used in this study; they were positioned in front of the animal as shown in Figure 1*B*. One was at shoulder level in the midsagittal plane with its front end 15 cm away from the animal. The remaining target buttons were placed at equal distances (12.5 cm) from the central one at the corners of an imaginary parallelepiped rotated in the horizontal plane 18° towards the performing arm. This placement of the stimulus elements allowed free, unobstructed movements from the center to peripheral targets in 8 directions at approximately equal angular intervals.

Movements of the animal's arm were recorded using a sonic tracking system (Chubbuck and Georgopoulos, 1984) in sessions separate from the electrophysiological recordings. A spark gap was attached to the monkey's wrist and was discharged every 20 msec. The sonic signal was picked up by at least 3 of 8 ultrasonic receivers placed at the corners of the workspace (Fig. 1*A*), and the *XYZ* coordinates of the gap were calculated from the sonic delays using a microprocessor-based system.

Animals and task. Two male rhesus monkeys (4–6 kg body weight) were used. They were trained to move their hand from the center to

Received Aug. 3, 1987; revised Dec. 10, 1987; accepted Dec. 10, 1987.

This work was supported by United States Public Health Service (USPHS) Grants NS17413 and NS07226, which we gratefully acknowledge. We thank Dr. Scott Zeger, Department of Biostatistics, The Johns Hopkins University, School of Hygiene and Public Health, for statistical advice; Mr. Paul B. Johnson for computer programming support; and Mr. Joseph T. Lurito for help during some of the experiments. The color illustration was produced using the Interactive Graphics Facility of the Department of Biophysics, The Johns Hopkins University School of Medicine. This facility was established and maintained by NIH and NSF grants and by a gift from the Richard-King Mellon Foundation. A.B.S. was a postdoctoral fellow, 1984–1987, partially supported by USPHS Grants MH18030 and NS21011. R.E.K. was a research associate, 1985–1987, partially supported by USPHS Grant NS20868.

Correspondence should be addressed to Apostolos P. Georgopoulos, Bard Laboratories of Neurophysiology, Department of Neuroscience, The Johns Hopkins University, School of Medicine, 725 North Wolfe Street, Baltimore, MD 21205.

[a] Present address: Division of Neurobiology, St. Joseph's Hospital and Medical Center, Barrow Neurological Institute, 350 West Thomas Road, Phoenix, AZ 85013.

[b] Present address: Department of Psychology, Psychology Building, Indiana University, Bloomington, IN 47405.

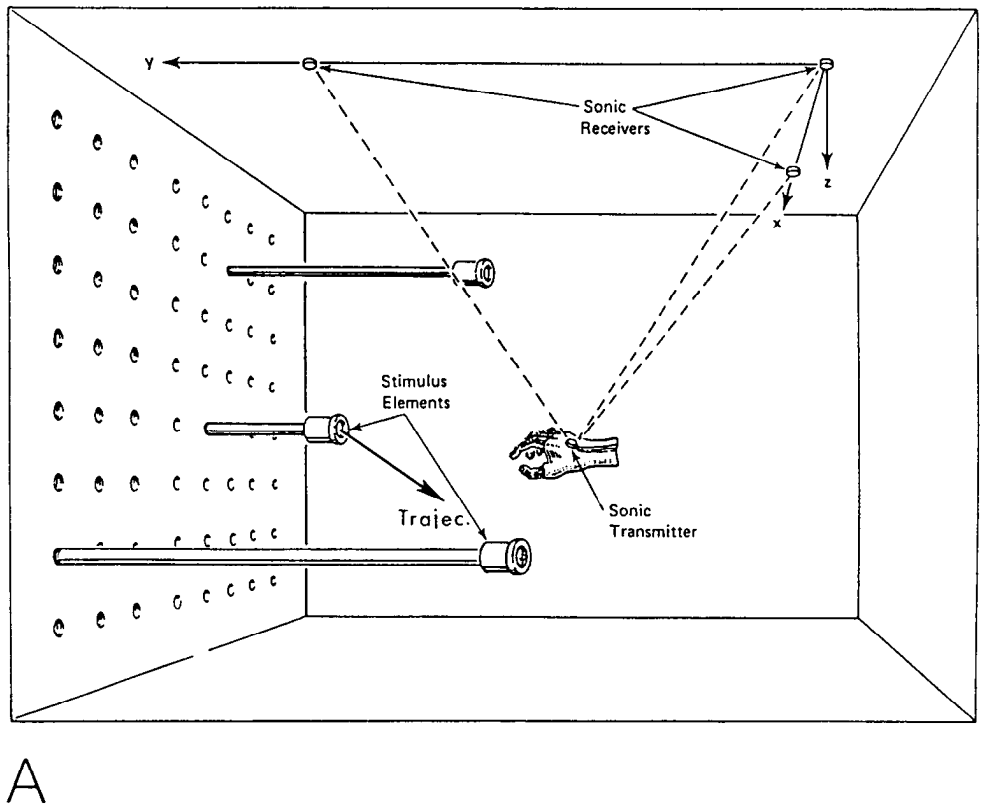

Figure 1. *A*, Schematic diagram of the apparatus. *B*, Layout of target lights.

peripheral lighted targets in a reaction time task as follows. The center light came on first, and the animal was required to depress and hold it for a variable period of time (at least 0.5 sec). Then, the center light went off, and 1 of the 8 peripheral lights came on. The animal was required to move towards and push the peripheral button for a variable period of time (at least 0.15 sec) to get a liquid reward. An upper limit of 1 sec was set for the reaction time and 1 sec for the movement time. All 8 targets were presented in a pseudorandom sequence before a target was repeated. Typically, 5–8 such repetitions of the 8 targets were obtained in a randomized block design (Cochran and Cox, 1957) for every cell studied.

Neuronal recordings. The electrophysiological methods and the surgical procedures have been described previously (Georgopoulos et al., 1982) and are summarized below. After the animals had been trained in the task, a circular recording chamber, 16 mm internal diameter, was placed over the motor cortex under general pentobarbital anesthesia and held in place by dental acrylic. On each recording day, the head was immobilized mechanically, and a Chubbuck mechanical microdrive (see Mountcastle et al., 1975) was attached to the fluid-filled and hydraulically sealed chamber. A glass-insulated Pt-Ir microelectrode was then lowered into the brain through the intact dura. Ordinarily, one microelectrode penetration was made per day. The location of each penetration on the surface of the brain was marked on a grid map of the chamber. Recording times were limited to 4–6 hr, after which the animal was returned to its home cage. Recording continued for about 30 d in each hemisphere. The electrical signs of discharge of single neurons in the motor cortex contralateral to the performing arm was recorded extracellularly. Action potentials of single neurons were identified by the criteria of Mountcastle et al. (1969) and separated using a differential amplitude discriminator. Every effort was made to isolate initially negative-going action potentials, an indication that the neuron was less likely to be damaged. A record was kept of the depth at which each cell was isolated along the length of a penetration, from the first cells recorded after entry into the cortex until entry into the white matter, as judged by the absence of initially negative-going potentials and the recording of purely positive (fiber) spikes. At the end of some penetra-

tions small lesions were made to facilitate the reconstruction of the penetration; typically a 3–4 μA current was passed through the tip of the microelectrode for 3 sec.

Once an action potential was isolated, an examination of the animal was carried out to determine whether the cell's activity was related to movements of a body part. The main reason for this examination was to select only arm-related cells for further quantitative study. This was necessary in order to avoid spurious results that could contaminate the database by studying task-related cells which would have been unrelated to the arm. For example, cells related to tongue or face movements were active during the task because the animals licked the reward tube continuously; such cells were not studied quantitatively.

Electromyographic (EMG) recordings. The EMG activity of the following muscles (Howell and Straus, 1933) was sampled in the task using intramuscular, Teflon-coated, multistranded, stainless steel wires: acromiodeltoid, spinal deltoid, pectoralis major, biceps, triceps, cervical trapezius, and extensor and flexor carpi radialis. The signals were recorded differentially with an approximate gain of 3000 and a bandpass of 100–500 Hz. The signals were then rectified and sampled every 10 msec. EMG recordings were done separately from neural recording sessions.

The EMG signals were recorded from a limited volume of the muscle in which the multistranded wires were inserted; no extensive sampling of other parts of a muscle was carried out. Therefore, the EMG data were regarded as qualitative observations and were not subjected to rigorous quantitative analysis.

Histological studies. At the end of the experiment the animals were killed with an overdose of pentobarbital administered intravenously. The head was immobilized mechanically in the same fashion as during the experiment, and the dura carefully removed as close to the circular border of the chamber as possible. Three pins were then inserted in a triangular array using a template attached to the stage of the microdrive. They were placed at known grid-map coordinates outside the area where penetrations were made. The brain was fixed in buffered formalin, embedded in celloidin, and sectioned every 20 μm. Each brain section was stained with thionin. The plane of sectioning was parallel to the insertion of the pins and as close as possible to being perpendicular to the central sulcus. The point of entry of penetrations into the brain was determined relative to the location of the pins using the grid map of the chamber. Some penetrations were also identified histologically from gliosis at the site of the small marking lesions (see above).

Data collection. A PDP 11/34 laboratory minicomputer was used to control the lights on the buttons, to record the opening and closure of the microswitches, and to collect analog (EMG), digital (*XYZ* coordinates of movement), and neural data. The latter were collected as interspike intervals with a resolution of 0.1 msec. All data were stored on-line in digital form. Neuronal data were displayed as rasters of spikes during the experiment.

Data analysis. Standard statistical and display techniques (Snedecor and Cochran, 1980; Draper and Smith, 1981) were used to analyze the data. Four epochs were distinguished for every trial. The *control time* (CT) extended from the time the animal pushed the center button at the onset of the trial until one of the peripheral targets was lighted; the *reaction time* (RT) was from that moment until the animal released the center button; the *movement time* (MT) followed and ended when the animal pushed the target button; finally, the RT and MT combined defined the *total experimental time* (TET). The mean frequency of discharge was calculated for each of these epochs, and an analysis of variance (ANOVA) was performed for every cell to determine whether the direction of movement had a statistically significant effect on the discharge rate. A significant F test at the 5% level distinguished cells with directional effects (see Results).

The activity of these cells was analyzed further using multiple linear regression to determine whether the discharge rate varied in an orderly fashion with the direction of movement in 3-D space. The following regression model was tested. Let X, Y, and Z be the positive axes of a Cartesian coordinate system with origin at the starting point of the movement (center button). The movement direction in 3-D space will be represented by a vector $\mathbf{M}$ of unit length which makes angles χ, ψ, and ω with axes X, Y, and Z, respectively. The vector $\mathbf{M}$ is specified by its x, y, and z components (m_x, m_y, m_z, respectively), where

$$m_x = \cos\chi, \quad m_y = \cos\psi, \quad m_z = \cos\omega$$

and

$$(m_x^2 + m_y^2 + m_z^2)^{1/2} = 1.$$

We adopt the notation that vectors are capitalized and in boldface. We used the following equation to relate cell activity to the direction of the movement:

$$d(\mathbf{M}) = b + b_x m_x + b_y m_y + b_z m_z, \tag{1}$$

where $d(\mathbf{M})$ is the discharge rate of a cell during movement $\mathbf{M}$, and b, b_x, b_y, and b_z are coefficients that vary from cell to cell. The values of these coefficients were estimated using multiple linear regression techniques (Draper and Smith, 1981). A significant F test in this regression ($p < 0.05$) distinguished those cells that fitted Equation 1.

Equation 1 implies that there is a particular movement vector $\mathbf{C}$ for which the frequency of cell discharge will be highest. The direction of this vector is the cell's *preferred direction,* which can be determined by estimating the components c_x, c_y, and c_z of the vector $\mathbf{C}$ from Equation 1 as follows:

$$c_x = b_x/k, \quad c_y = b_y/k, \quad c_z = b_z/k,$$

where

$$k = (b_x^2 + b_y^2 + b_z^2)^{1/2}.$$

Substituting in Equation 1, we get

$$\begin{aligned} d(\mathbf{M}) &= b + kc_x m_x + kc_y m_y + kc_z m_z \\ &= b + k(c_x m_x + c_y m_y + c_z m_z) \end{aligned} \tag{2}$$

Using the dot product relationship between $\mathbf{C}$ and $\mathbf{M}$, we have

$$c_x m_x + c_y m_y + c_z m_z = \mathbf{C}\cdot\mathbf{M} = |\mathbf{C}||\mathbf{M}|\cos\Theta_{CM}, \tag{3}$$

where Θ_{CM} is the angle formed by the cell's preferred direction $\mathbf{C}$ and the direction of movement $\mathbf{M}$ and where $|\mathbf{C}|$ and $|\mathbf{M}|$ are the lengths of vectors $\mathbf{C}$ and $\mathbf{M}$, respectively. Substituting Equation 3 into Equation 2, we get

$$\begin{aligned} &d(\mathbf{M}) = b + k|\mathbf{C}||\mathbf{M}|\cos\Theta_{CM} \quad \text{or} \\ &d(\mathbf{M}) = b + k\cos\Theta_{CM} \end{aligned} \tag{4}$$

because both $|\mathbf{C}|$ and $|\mathbf{M}| = 1$, since $\mathbf{C}$ and $\mathbf{M}$ are vectors of unit length. Equation 4 will be referred to as the *directional tuning function* in the remainder of the paper. It follows from this equation that the discharge rate, $d(\mathbf{M})$, will be highest with movements in the preferred direction, that is, when $\mathbf{M}$ and $\mathbf{C}$ coincide ($\Theta_{CM} = 0°$, $\cos\Theta_{CM} = 1$), lowest when $\mathbf{M}$ is opposite to $\mathbf{C}$ ($\Theta_{CM} = 180°$, $\cos\Theta_{CM} = -1$), and in between with movements in intermediate directions ($0° < \Theta_{CM} < 180°$, $1 > \cos\Theta_{CM} > -1$). Equation 4 can potentially yield negative values for $d(\mathbf{M})$; in that case, $d(\mathbf{M})$ is set to zero, for discharge rates can only take values of greater or equal to zero. A logarithmic model of the form

$$d(\mathbf{M}) = \exp(b' + k'\cos\Theta_{CM})$$

or, equivalently,

$$\log_e d(\mathbf{M}) = b' + k'\cos\Theta_{CM}$$

would force all predicted values to be positive (b' and k' are new constants). However, we chose to stay with the model of Equation 4 as it does not involve any transformation of the discharge rates to another scale.

The preferred direction estimated as described above was based on discharge rates averaged over 5–8 repetitions. It was possible to estimate the variability of the preferred direction from repetition to repetition, for the experiment was carried out in a randomized block design (see above); that is, all peripheral targets were presented within a repetition, which, therefore, comprised movements in all 8 directions. The method was as follows. First, the preferred direction was calculated for each of the available 5–8 repetitions. Then, the variability among these directions was estimated by calculating the spherical variance, S^* (Mardia, 1972, p. 219):

$$S^* = (n - R)/n, \quad 0 \le R \le n, \quad 0 \le S^* \le 1, \tag{5}$$

where n is the number of directions (one for each repetition) and R is the length of the resultant. S^* can vary from 0 to 1: a value near 1 indicates that the constituent directions differ greatly, that is, that the directional variability is very high; on the other hand, a value near 0 indicates that the directions are very similar, that is, that the directional variability is very low.

In a previous study in 2-D space (Georgopoulos et al., 1982), we defined an index of directional modulation, I_d, as a normalized measure of the depth of directional tuning. The same measure applies in the

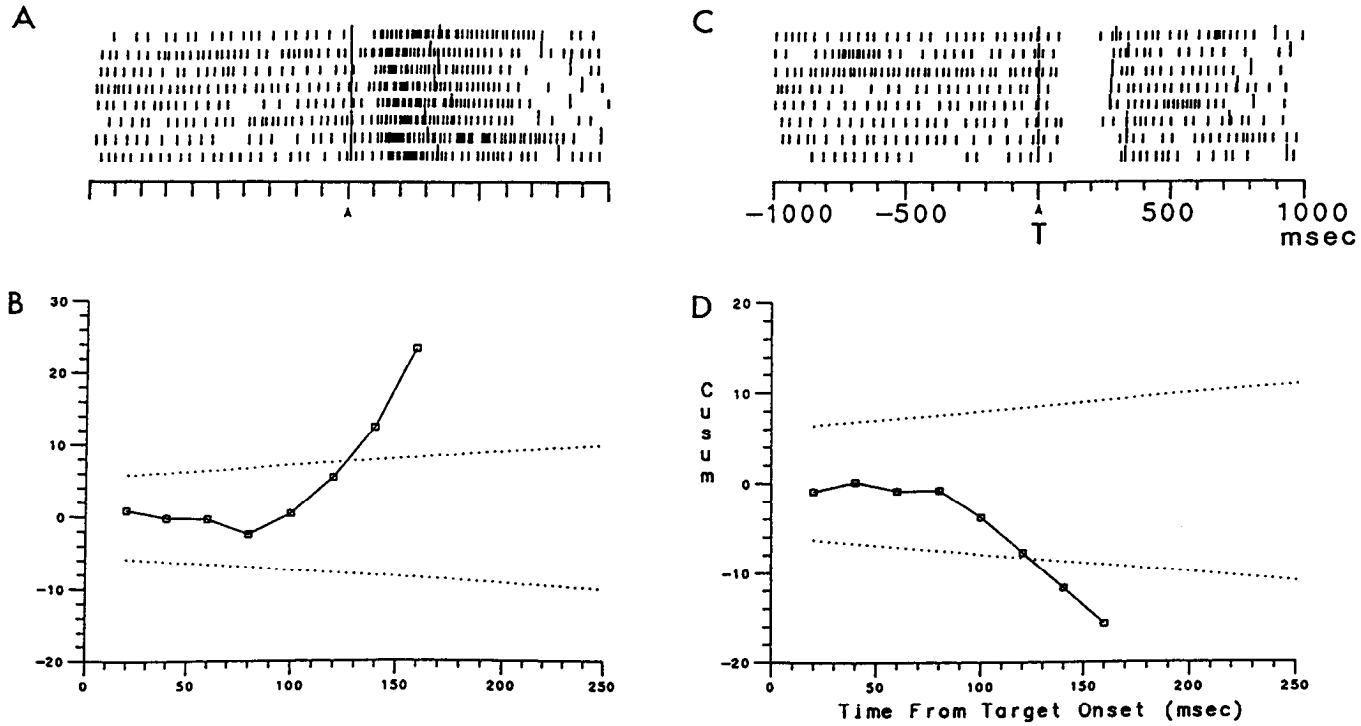

Figure 2. Latency measurement: *A* and *C*, impulse activity (*short bars*) of the same cell during movements in 2 different directions; rasters of 8 repeated trials are aligned to the onset of the target (*T*); 2 successive *longer bars* indicate the onset and the end of movement, respectively. *B* and *D*, CUSUM (*solid line*) and upper and lower boundaries (*dotted line*).

present 3-D case, as follows:

$$I_d = k/b \qquad (b > 0) \tag{6}$$

Determination of neuronal onset times. The latency of change in single-cell activity from the time of onset of a peripheral target was determined using a cumulative sum technique (Ellaway, 1977, 1978) combined with sequential significance testing (Armitage, 1975), as follows. (1) For each of the 8 movement directions, peristimulus time histograms were constructed by averaging across repetitions using a 20 msec bin width, starting 500 msec (=25 bins) before the onset of the target light. (During this control period, the monkey was pushing the center button.) (2) The mean control rate per bin was calculated for the first 25 bins. This provided the background rate from which changes in activity were calculated and summed. (3) The SD, σ, of the 25 control bins was also calculated. This provided the variability used to construct boundaries to test the significance of accumulated changes in discharge rate with time. (4) Next, a running cumulative sum (CUSUM) was computed of the differences between the mean control rate and successive bin rates starting from the time of target onset and continuing forward. On the null hypothesis that these rates do not differ from the control rate, the value of the CUSUM should tend to be zero. However, fluctuations of the CUSUM above or below zero will occur by chance, and it is the purpose of the sequential technique to test whether a particular deviation from zero is statistically significant. This was accomplished as follows. (5) Expected chance levels of the CUSUM were calculated for every CUSUM value, that is, for every bin contributing a difference to the running CUSUM. Two boundaries were thus generated: an upper (positive) and a lower (negative). When the CUSUM became greater than the upper, or less than the lower, boundary, a significant increase or decrease, respectively, in the bin rate was deemed to have occurred, compared to the mean control rate. The boundaries were functions of 3 variables. The first was the variability of the differences being summed. We assumed that the variability of the differences of the successive bin rates from the mean control rate, starting from the target onset and until the first significant change was detected, was not different from that observed in the control period. Therefore, the SD, σ, of that period was used. The second factor related to how many times the testing had been performed. It has been shown that the probability that a significant change will be found by chance alone increases as a test of significance is performed repeatedly, either on the CUSUM or on successive, non-summed measurements (see Armitage, 1975, pp. 27–31). Therefore, for proper sequential (or repeated) testing, the boundaries will have to expand as the bin number increases. Finally, the third factor related to the level of the significance testing desired (e.g., 5% or 1%), the critical value of change to be detected, and the statistical plan involved. There are basically 2 kinds of plans: open and closed. In the open plans, repeated testing can continue indefinitely; for this reason they are inappropriate for this application, because the spike trains were of finite length. Closed plans involve repeated testing for a certain number of times, depending on the extent of the data available and the critical difference to be detected. Closed, restricted plans with known variability were used in the present analysis.

The following equations for the upper (U) and lower (L) boundaries were used (Armitage, 1975, p. 97):

$$U: \quad y = 5.2\sigma + 0.35\sigma n,$$
$$L: \quad y = -5.2\sigma - 0.35\sigma n,$$

where σ was as defined above and n is the bin number, being incremented from the time of target onset. The constants 5.2 and 0.35 relate to the plan, the significance level chosen, and the number of repeated tests allowed: they correspond to a closed, restricted plan with 2-sided overall significance level, $2\alpha = 0.033$; power, $1 - \beta = 0.95$; critical value of change to be detected, $\delta_1 = 0.7$; and an approximate maximum of 36 times of testing (see Table 5.3 in Armitage, 1975, p. 101). Given the 20 msec bin width used in this analysis, 36 times of testing corresponded to 720 msec from the time of target onset. The testing was stopped when one of the following 3 events occurred. (1) Either boundary was crossed by the CUSUM *and* the 2 subsequent bins showed changes from the control rate in the same direction (increase or decrease). The latter requirement was added as a measure of consistency of the change observed. (2) The spike train ended. Or, (3) 36 consecutive tests were performed without the CUSUM crossing either boundary. In that case, a change could have occurred later in time but was not considered. The maximum time of 720 msec allowed for this testing was close to the average time elapsed from the onset of target until the end of the movement in all movements obtained (mean = 730 msec).

An example of the technique used is shown in Figure 2. Panel *A* shows 8 spike trains corresponding to movements to the same target. In panel *B*, the CUSUM is plotted, starting from the first bin following target onset, together with the upper and lower boundaries. The CUSUM crossed the upper boundary on the 7th bin, which gives an estimate of 140 msec as the latency of increase in cell activity. The rates of the 2

subsequent bins were greater than the control rate. Figure 2, *C, D,* illustrates a case in which a decrease in activity was detected. In general, this method for calculating onset times took into account the fact that repeated significance tests were performed and yielded more conservative results than those obtained using repeated t tests. The same technique was used to detect the first changes in EMG activity.

Results

Wrist trajectories

The animals moved from the center to peripheral lights in a stereotyped fashion. A typical example of 8 trajectories to one of the targets is shown in Figure 3. Average RT, MT, and TET epochs for all movements performed (n = 28,800) were (mean ± SD) 300 ± 75 msec, 431 ± 227 msec, and 730 ± 240 msec, respectively.

EMG studies

All muscles studied were active in the task, and it is reasonable to suppose that other muscles were also involved. Figure 4 shows an example of EMG records obtained from the acromiodeltoid muscle during movements in the 8 directions studied. The flexor and extensor muscles of the hand were continuously active during the movement, probably to fixate the wrist. Movements in different directions were accomplished by concomitant changes in the activity of several muscles. An example is shown in Figure 5.

Neuronal recordings

Five hundred sixty-eight arm-related cells were studied in the task during 100 microelectrode penetrations into the motor cortex of 4 hemispheres in 2 monkeys. The approximate location of the entry points of these penetrations on the cortical surface is illustrated in Figure 6. All cells included in this study discharged in relation to proximal arm movements (at the shoulder and/or elbow), as determined by examination of the animal outside the behavioral task (see Materials and Methods). The location of penetrations with proximal arm cells on the cortical surface (Fig. 6) is similar to that described before (Georgopoulos et al., 1982) and coincides approximately with the outline of the proximal arm area in the map of Woolsey et al. (1950). Of the cells studied, 154 were recorded in the first, 124 in the second, 183 in the third, and 107 in the fourth hemisphere. Finally, the distribution of the depth at which cells were recorded (data not shown) suggested that the cortex was sampled throughout its depth.

Single-cell database

An ANOVA was performed to identify the cells whose discharge rate varied significantly with the direction of movement. For the latter group, a multiple linear regression was then performed to identify the cells whose discharge rate varied in the way described by the tuning function (Eq. 4). The following groups of cells were distinguished. (1) *Directionally tuned* (475/568, 83.6%, TET epoch) cells showed both significant changes in activity with movement direction (ANOVA, F test, $p < 0.05$) and a good fit of the tuning function (multiple regression, F test, $p < 0.05$). The percentage of tuned cells was 61.1 and 84.7 for the RT and MT epochs, respectively. (2) *Irregular* (31/568, 5.5%, TET epoch) cells exhibited activity that differed significantly among the different directions but did not fit the tuning function. The percentage of irregular cells was 0.9 and 4.9 for the RT and MT epochs, respectively. Finally, (3) *nondirectional* (62/568, 10.9%, TET epoch) cells demonstrated activity during the task that did not differ significantly among the different directions. The percentage of nondirectional cells was 38.0 and 10.4 for RT and MT epochs, respectively.

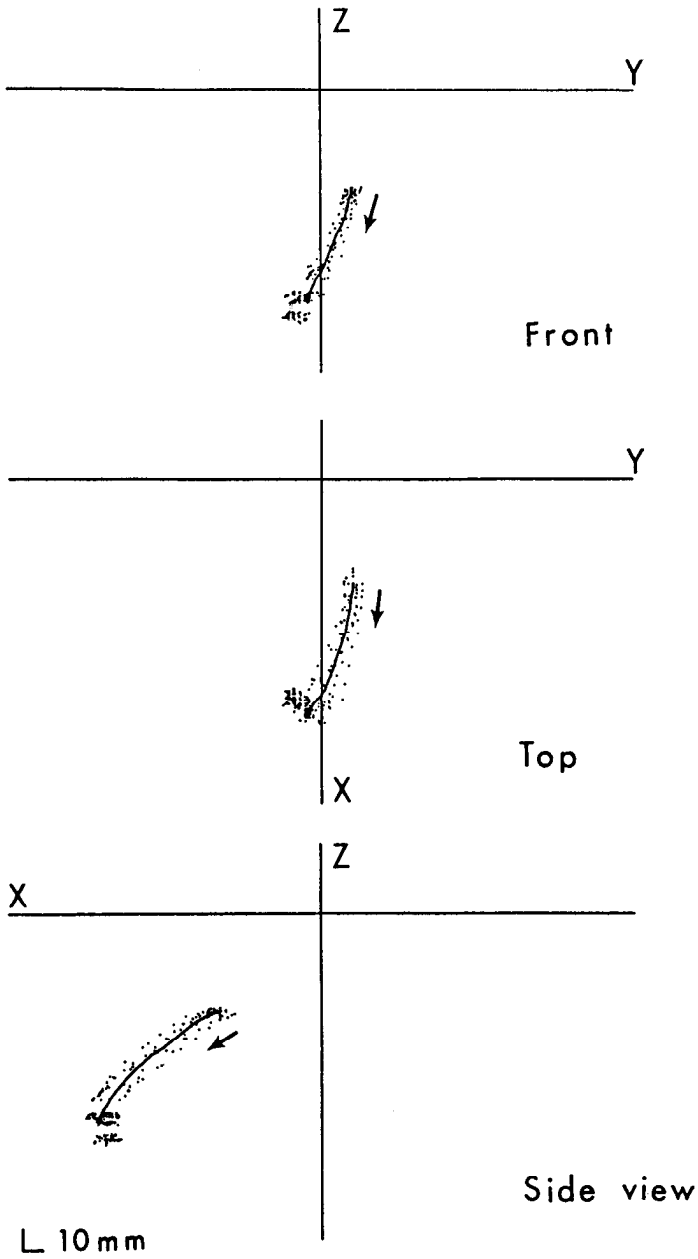

Figure 3. Average trajectories (*solid line*) of 8 movements to the lower, left, and forward target. Dots are 20 msec position samples of individual trajectories.

Directional changes in cell activity were observed frequently before the earliest changes in EMG activity. Below, we illustrate first the findings from single neurons and then summarize the findings from all directionally tuned cells. We also describe the results of the quantitative analysis for the TET epoch because, frequently, the neuronal response occupied parts of both the RT and the MT.

Results from single neurons

Figure 7 shows in raster form the variation in activity of a single cell with the direction of movement. It can be seen that cell

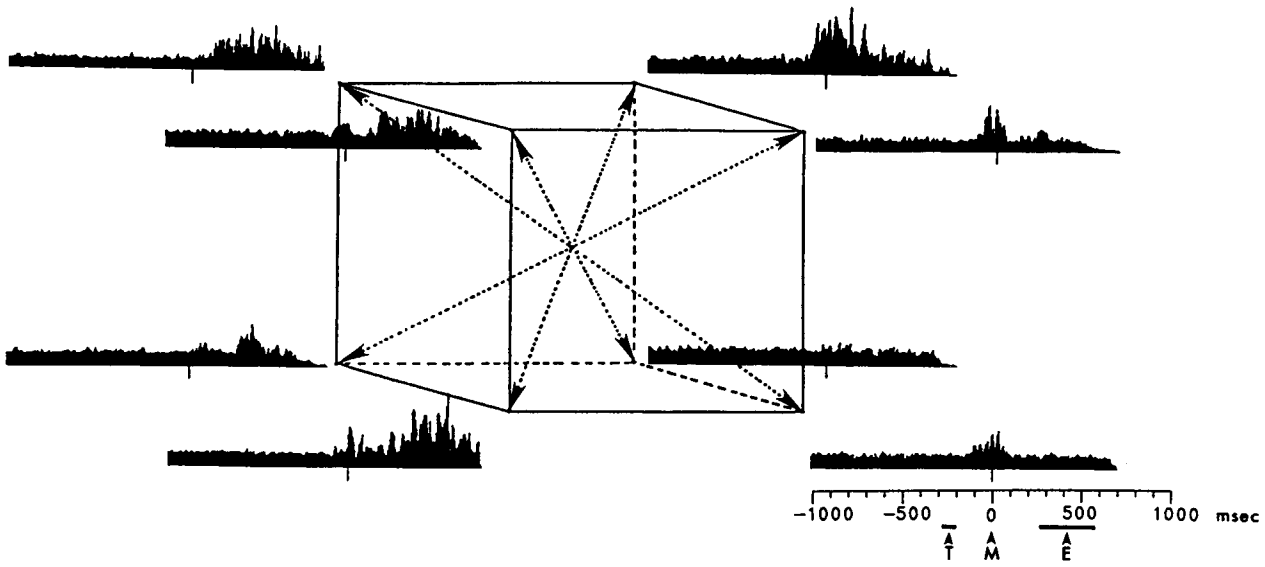

Figure 4. EMG activity of acromiodeltoid muscle during movements of different directions (*arrows*). Histograms are averages of 8 trials aligned to the onset of movement (*M*). *T*, average (±1 SD) onset of target; *E*, average (±1 SD) end of movement. Right arm.

discharge was highest with movements to the left and downwards and decreased with movements in other directions. The schematic diagram at the center of the figure shows a 3-D plot of the movement directions tested. A statistically significant variation in the discharge rate with the direction of movement was found (ANOVA, F test, $p < 0.001$). The variation of the average (across repetitions) frequency of discharge with the direction of movement was described by the following equation, which corresponds to Equation 1 above:

$$d(\mathbf{M}) = 41.9 - 6.93m_x - 29.90m_y - 19.85m_z, \qquad (7)$$

where d is the discharge rate, and m_x, m_y, m_z are the components of the movement vector, as defined in Materials and Methods. The F test for the multiple regression (Eq. 7) was statistically significant ($p < 0.02$). The tuning function for that cell was

$$d(\mathbf{M}) = 41.90 + 36.55 \cos \Theta_{CM}, \qquad (8)$$

where Θ_{CM} is the angle formed by the direction of movement, **M**, and the cell's preferred direction, **C**. The linear relation between the cosine of this angle and the discharge rate (Eq. 8) is shown in Figure 8. It can be seen that the observed discharge rates fall on either side of the fitted line in a nonsystematic fashion. The preferred direction, **C**, is specified by its components

$$c_x = -0.190, \qquad c_y = -0.818, \qquad c_z = -0.543.$$

Finally, the index of directional modulation, I_d, for this cell was

$$I_d = 36.55/41.9 = 0.872.$$

The tuning function described by Equation 8 above implies that cell discharge will be highest with movements in the preferred direction, will decrease gradually according to the cosine function with movements in directions farther and farther away from the preferred one, and will be lowest for movements in the opposite direction. This predicted variation in cell discharge with the direction of movement in 3-D space describes the "tuning volume," which is illustrated in Figure 9 for the cell whose rasters are shown in Figure 7. The predicted frequency of discharge for a particular movement direction is proportional to the length of the line drawn from the origin of the axes (corresponding to the origin of the movements) to the surface of the solid in the direction of the movement. Figure 10 illustrates the general case of a section of a tuning volume through the axis of the preferred direction. This is actually a 2-D plot of the tuning function realized in the plane of section, in accordance with Equation 4 above. The tuning volume can be derived from this plot by orienting the latter in space according to the preferred direction and rotating it 360° around the axis of the preferred direction.

Figure 11 shows the impulse activity, during the task, of a nondirectional cell (ANOVA, F test, $p < 0.3$). It can be seen that the cell activity changed appreciably after the onset of the target, but the intensity of activation did not vary with movement direction.

Summary of results from all directionally tuned cells

Preferred directions. The preferred directions of the cells studied ranged over the whole 3-D directional continuum. Their distribution is shown in Figure 12*A* as a 3-D plot and in Figure 12*B* as an equal-area projection plot. All data refer to the right arm. In Figure 12*B*, squares and crosses are points from the upper and lower hemispheres, respectively. The plot is produced as follows (Watson, 1983, p. 22). First, the preferred directions are considered as vectors of unit length with origin at the center of a unit sphere. Second, the points where these vectors terminate are marked on the surface of the sphere. Finally, the surface of each of the 2 (upper and lower) hemispheres is projected onto a circular plane in such a way that areas on the hemisphere are projected to regions of equal area on the plane.

In the plot of Figure 12*B* the center of the imaginary unit sphere is at the origin of the movement. Preferred directions pointing above or below the equatorial plane are indicated by squares and crosses, respectively. Points near the center indicate directions towards the poles, whereas points near the outermost circle indicate directions towards the equator. The 4 major radii correspond, respectively, to movement directions straight for-

ward away from the body (radius toward 12 o'clock), straight toward the body (6 o'clock), and toward the ipsilateral (3 o'clock) or contralateral (9 o'clock) side of the performing arm. It can be seen that the preferred directions are distributed over the whole range of the 3-D directional continuum in an approximately uniform fashion [null hypothesis of uniformity not rejected, Rayleigh test (Watson, 1956), $p < 0.9$]. It seems that there is a somewhat higher density of points towards the equatorial region (outer part of the plot) and straight forward (around 11 o'clock). It is not clear whether these local concentrations are due to variation in sampling of the cells studied or represent true, if subtle, departures from uniformity.

The distribution of the spherical variance, S^*, obtained for each of the 475 directionally tuned cells was heavily skewed towards small values (data not shown); the median value of S^* was 0.066, indicating that the preferred directions obtained from different repetitions for a particular cell were very similar.

Tuning function parameters. The tuning function described by Equation 4 is completely specified by the 2 parameters b and k. The parameter b is the *true* Y-intercept in the linear plot described by the tuning function (when $\cos \Theta_{CM} = 0$). The parameter k is the slope of the line described by the tuning function; since $\cos \Theta_{CM}$ is a pure number, the units of k are in impulses per second. The value of k equals the highest predicted cell discharge (above the Y-intercept, b) which occurs when the movement is in the cell's preferred direction (that is, when $\cos \Theta_{CM} = 1$). Figure 13, *A, B,* shows the distributions of b and k, respectively; Figure 13*C* is a scatter plot of k versus b in a log-log scale. (This scale was chosen because in the untransformed plot the variability increased with the magnitude of b and k.) The 2 parameters are positively correlated ($N = 475$; $R = 0.859$, $p < 0.001$, after log-log transformation; $R = 0.759$, $p < 0.001$ for untransformed scale).

Depth of directional modulation. The distribution of the index of directional modulation, I_d, for all directionally tuned cells is shown in Figure 14. The distribution is skewed with the mode around $I_d = 0.6$.

Predicted discharge rates. The discharge rates predicted by Equation 4 were compared with the actually observed ones for the 8 movement directions tested using an analysis of the residuals, that is, of the differences between predicted and actually observed rates. We wanted to know whether the predicted discharge rates for some directions were systematically more, or less, accurate than for other directions. For that purpose, we generated 8 frequency distributions of the residuals ($N = 475$), one for each movement direction. These distributions (data not illustrated) were symmetric about a mean of approximately zero and had approximately the same spread. These results indicate that discharge rates were predicted with approximately the same accuracy for all movement directions and that there were no systematic deviations in the overall predictions from the actually observed ones.

A different question concerns the sign of the predicted rates. Equation 4 predicts negative discharge rates for some directions when $k > b$; for example, when the movement is in a direction opposite to the preferred direction, that is, when $\Theta_{CM} = 180°$ and $\cos \Theta_{CM} = -1$. This was true for 127/475 (26.7%) of the cases; this proportion fell to 43/475 (9.1%) for movement directions made at $\pm 135°$ away from the preferred direction ($\cos \Theta_{CM} = -0.707$). Obviously, negative discharge rates are unrealizable in practice because the lowest possible rate in the spike train is zero. Indeed, for subsequent analyses (see Georgopoulos et al., 1988) we assumed the rate to be zero when a negative value was predicted.

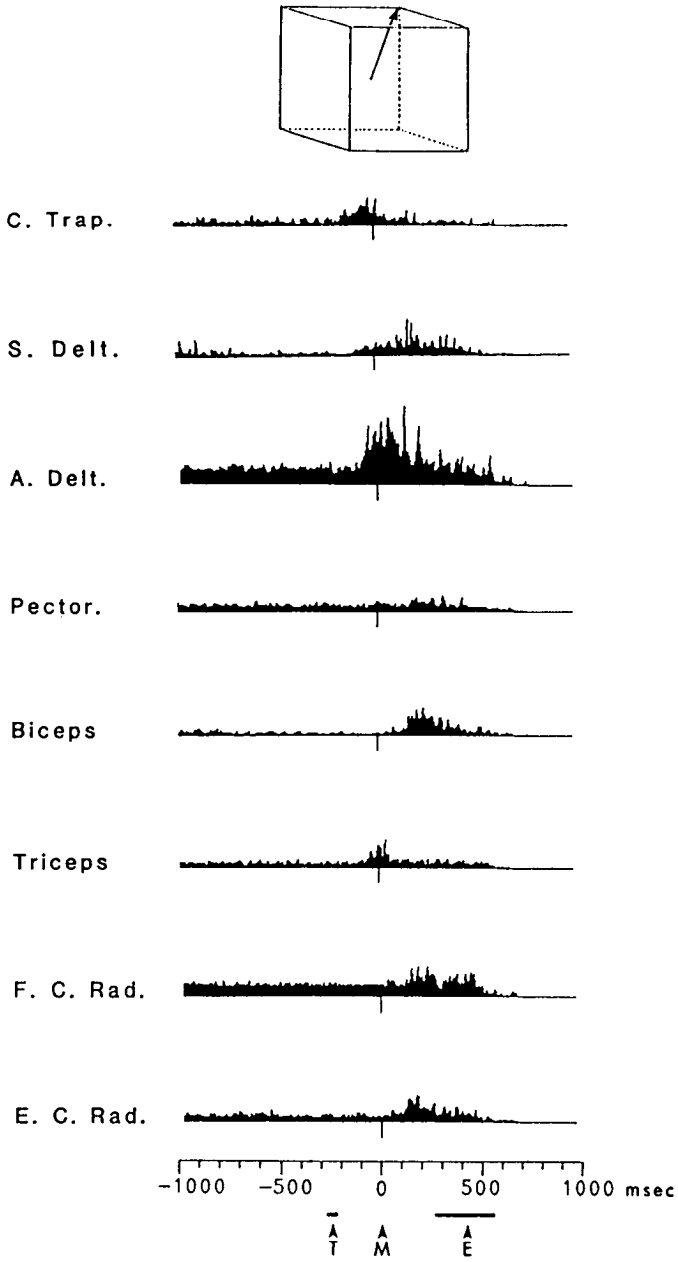

Figure 5. EMG activity of 6 proximal muscles during movements to the upper, right, and backward target. Right arm. Abbreviations as in Figure 4. *C. Trap.*, cervical trapezius; *S. Delt.*, spinal deltoid; *A. Delt.*, anterior deltoid; *Pector.*, pectoralis; *F. C. Rad.*, flexor carpi radialis; *E. C. Rad.*, extensor carpi radialis.

Latencies of changes in cell and EMG activity

The distribution of the latencies of increase in cell activity is shown in Figure 15 (solid line). The plot is based on 2584 increases detected as the first change in cell activity among 4544 determinations performed (568 cells × 8 movement directions). The first appreciable increases in discharge occurred 60–80 msec following the presentation of the target. The peak of the distribution was at the 120–140 msec bin. Given that, on average, the movement began 300 msec after target onset, 71% of the increases in activity occurred before movement onset. The la-

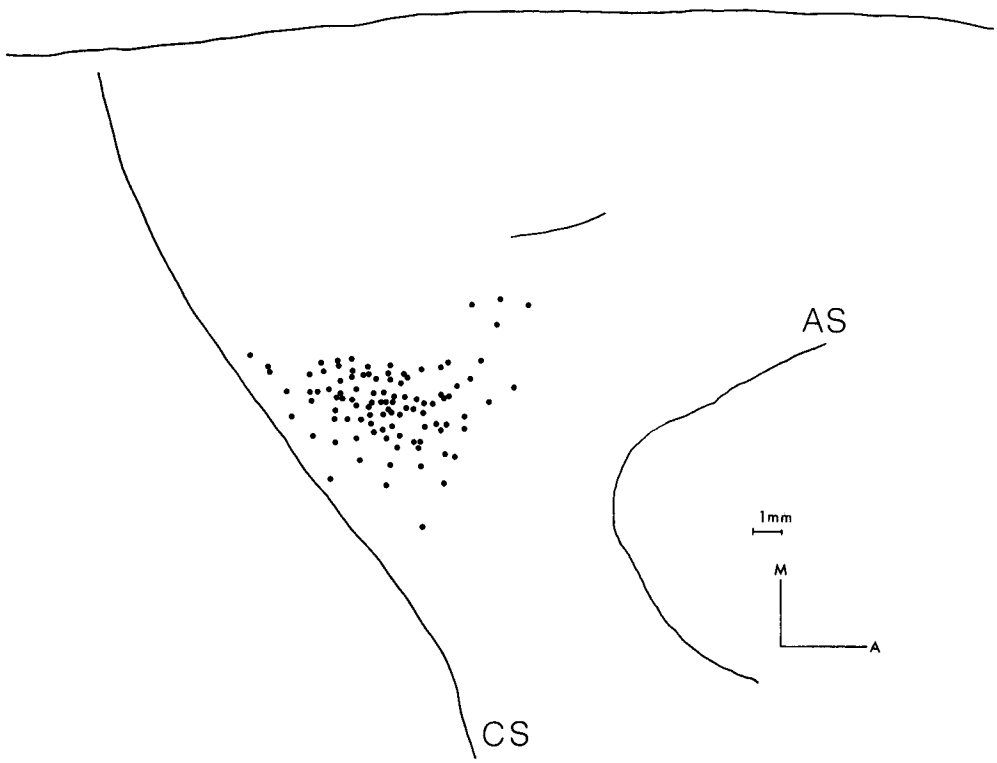

Figure 6. Diagram showing the location on the cortical surface of entry points of penetrations ($n = 100$) in which cells related to proximal arm movements were recorded. Data from 4 hemispheres are plotted on an outline of a right hemisphere. *CS*, central sulcus; *AS*, arcuate sulcus; *A*, anterior; *M*, medial.

tency distributions corresponding to particular movement directions (data not shown) did not differ significantly from one another (Kolmogorov-Smirnov test).

The distribution of first increases in EMG activity is also shown in Figure 15 (dotted line). The plot is based on 43 increases detected as the first change in EMG activity among 48 determinations performed [$n = 6$ proximal muscles (acromiodeltoid, spinal deltoid, pectoralis, biceps, triceps, cervical trapezius) × 8 directions = 48]. It can be seen that the first changes occurred at the 160–180 msec bin following target onset, corresponding to 140–160 msec preceding the average onset of movement. The cell latency distribution was significantly earlier in time than the EMG latency distribution (Kolmogorov-Smirnov test, 2-tailed, $p < 0.001$).

Decreases in activity (data not shown) were observed less frequently than increases. This was probably due to the fact that 172/568 (30%) of the cells studied did not discharge tonically or discharged at very low rates (<2 imp/sec) preceding the stim-

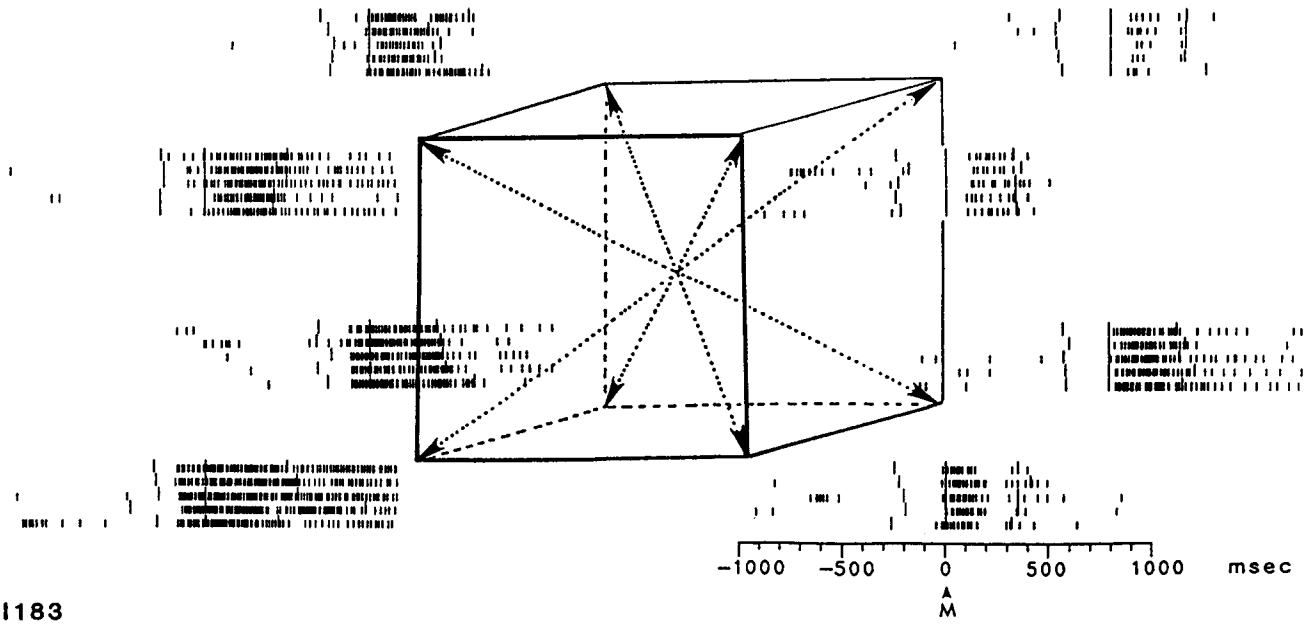

Figure 7. Impulse activity (*short bars*) of a directionally tuned cell with movements in different directions (*arrows*). Rasters of 5 repeated trials for every movement direction are aligned with the onset of movement (*M*). *Longer bars* preceding and following the movement onset indicate the onset of the target and the end of the movement, respectively.

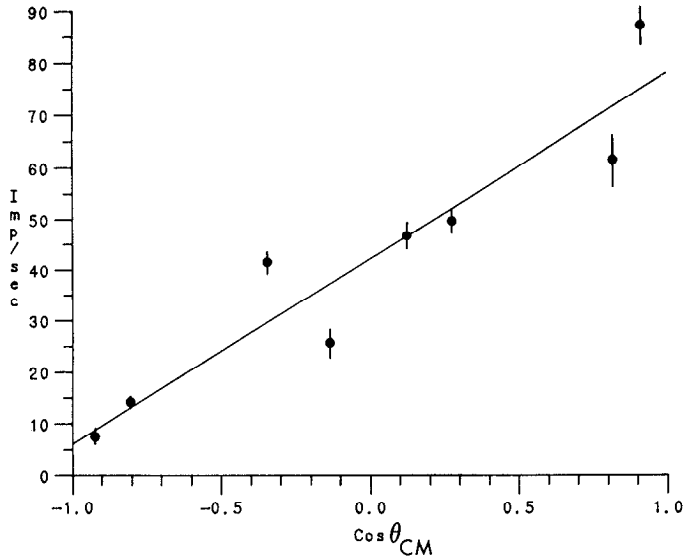

Figure 8. Mean discharge rate versus cos Θ_{CM} (see text). Data from cell whose impulse activity was illustrated in Figure 7. Vertical bars are ±1 SD.

ulus onset, and therefore it was difficult or impossible to detect a decrease in activity. When the latencies were determined for the subset of cells whose tonic rate during the control period was 10 imp/sec or more, increases were observed approximately 1.2 times as frequently as decreases. This is probably close to the true ratio and indicates a small preponderance of increase over decrease in activity as the first change in discharge rate. The distribution of decreases in the whole sample or in the subset described above was very similar to that of the increases, but it lagged in time by approximately 40 msec at the level of

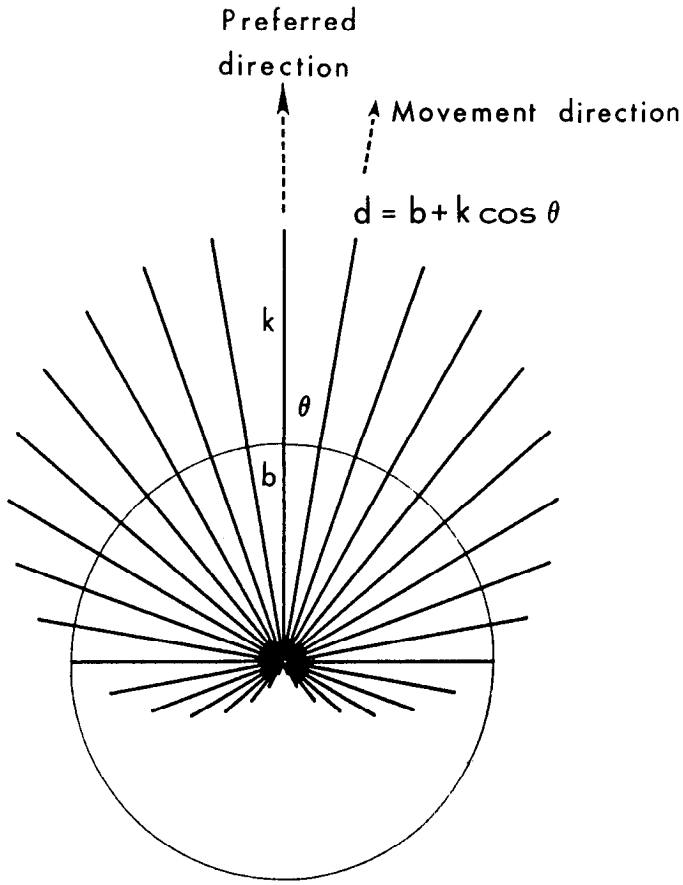

Figure 10. Cross section of tuning volume through the preferred direction. Length of a line indicates the predicted discharge rate with movements in the direction of the line. Equation is the tuning function (see Eq. 4 in text).

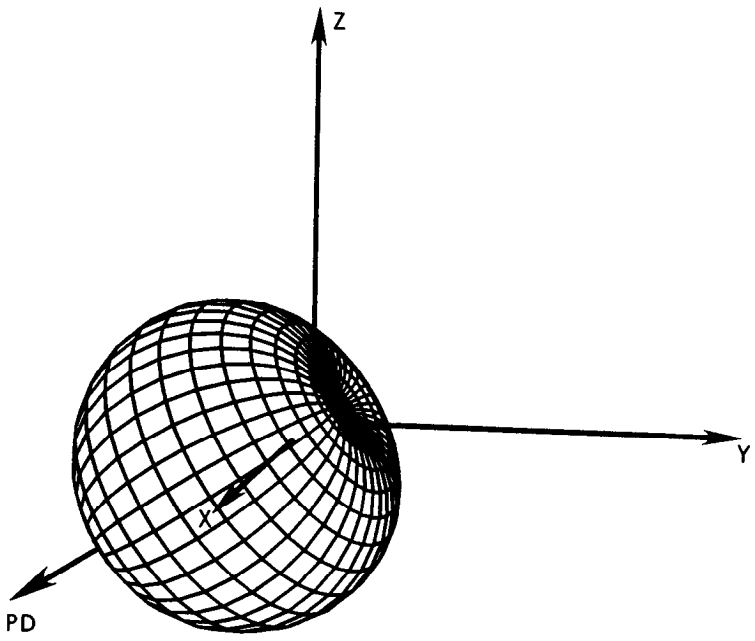

Figure 9. Predicted tuning volume of cell whose data are illustrated in Figures 7 and 8. *PD,* preferred direction.

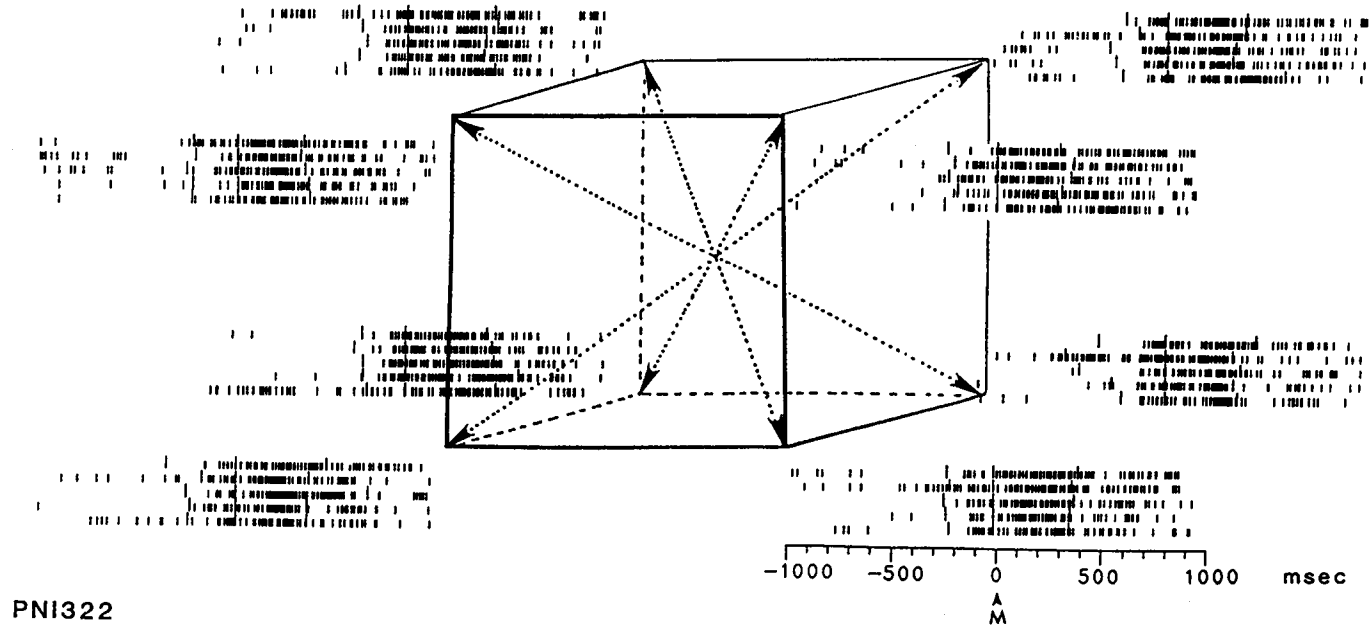

Figure 11. Impulse activity of a nondirectional cell. Abbreviations as in Figure 7.

the medians. This time lag was statistically significant (Kolmogorov-Smirnov test, 2-tailed, $p < 0.001$).

Discussion

A salient finding of the present study is that the frequency of discharge of many arm-related cells in the motor cortex varies in an orderly fashion with the direction of arm movement in 3-D space. The broad tuning function that describes this relation in 3-D space is radially symmetric with respect to the axis of the preferred direction and has a maximum in that preferred direction. The form of the tuning function is similar to that used for 2-D arm movements (Georgopoulos et al., 1982). Therefore, it appears to describe in a generalized, quantitative fashion the directional properties of motor cortical cells. It should be noted that in the experimental design used in the present study the direction of movement and the target (endpoint) of the movement in space were confounded. In a previous study in which these 2 factors were dissociated in 2-D space, the changes in motor cortical cell activity were found to be related to the direction of the movement and not to its endpoint (Georgopoulos et al., 1985). We summarize below the results of previous studies of cortical cell activity in relation to motor variables and during reaching, and focus on the direction of movement as the specified parameter.

Latencies of changes in cell activity

Most cells (71%) were activated before the onset of movement, and the distribution of initial increases in activity led that of decreases by about 40 msec. A salient finding was that the distributions of onset times were very similar and statistically indistinguishable among the 8 directions of movement studied. This suggests that the underlying mechanisms by which motor cortical cells become engaged in time, as an ensemble, during the initiation of movement are similar with respect to the direction of movement.

The first appreciable increases in activity (in terms of number of cells involved) occurred at about 60 msec following target onset, and the distribution peaked at 120–140 msec. Similar results were obtained in a previous study (Georgopoulos et al., 1982), and also by Murphy et al. (1982, 1985) for cells related to shoulder and/or elbow movements. This early engagement of the motor cortex in the initiation of visually aimed reaching movements suggests that these movements may not require a large amount of information processing before their initiation. Indeed, this was proposed previously based on the results of behavioral studies (Georgopoulos et al., 1981).

A different question concerns the pathways through which this early engagement of the motor cortex in reaching could be effected. The various possibilities have been reviewed in detail by Humphrey (1979), but no definite statements can be made.

Relations of motor cortical cell discharge to motor variables

Most studies of motor cortical discharge during the past 2 decades have been focused on the relations between single-cell activity and the magnitude of force exerted by the hand, especially under isometric conditions (see Evarts, 1981, for a review). It is now known that the discharge rate of motor cortical cells varies with the magnitude of force and that cells with higher thresholds are recruited at progressively higher forces (Hepp-Reymond et al., 1978). The variation of cell activity with force is observed most clearly for cells that probably make monosynaptic connections onto motoneurons in the spinal cord (Cheney and Fetz, 1980). Moreover, Fromm (1983) has provided evidence that this variation in cell activity might relate to the intensity of muscular contraction rather than to force intensity itself.

It should be noted that these relations have been investigated only for joints distal to the shoulder. In fact, given the finding that these relations are clearly observed only in cells possessing monosynaptic connections to motoneurons (Cheney and Fetz, 1980), it is doubtful whether they would be observed clearly for the shoulder joint, for only a few connections to proximal muscle

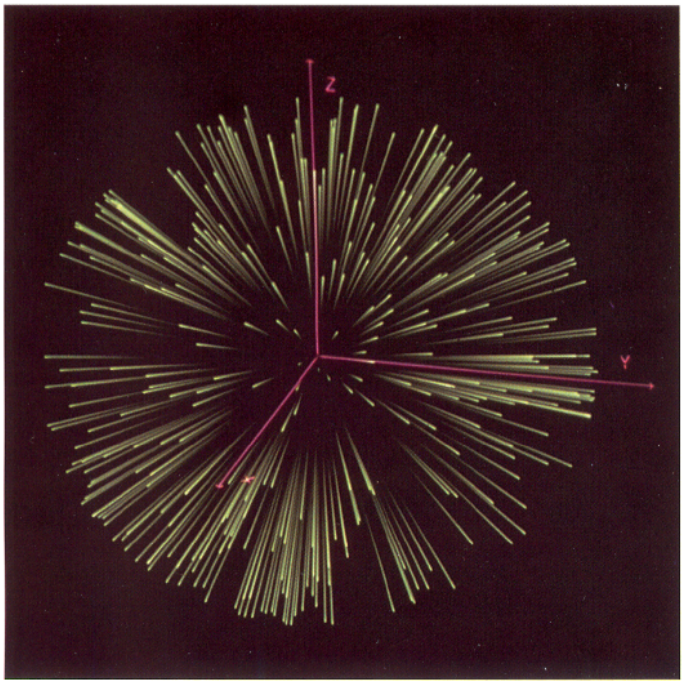

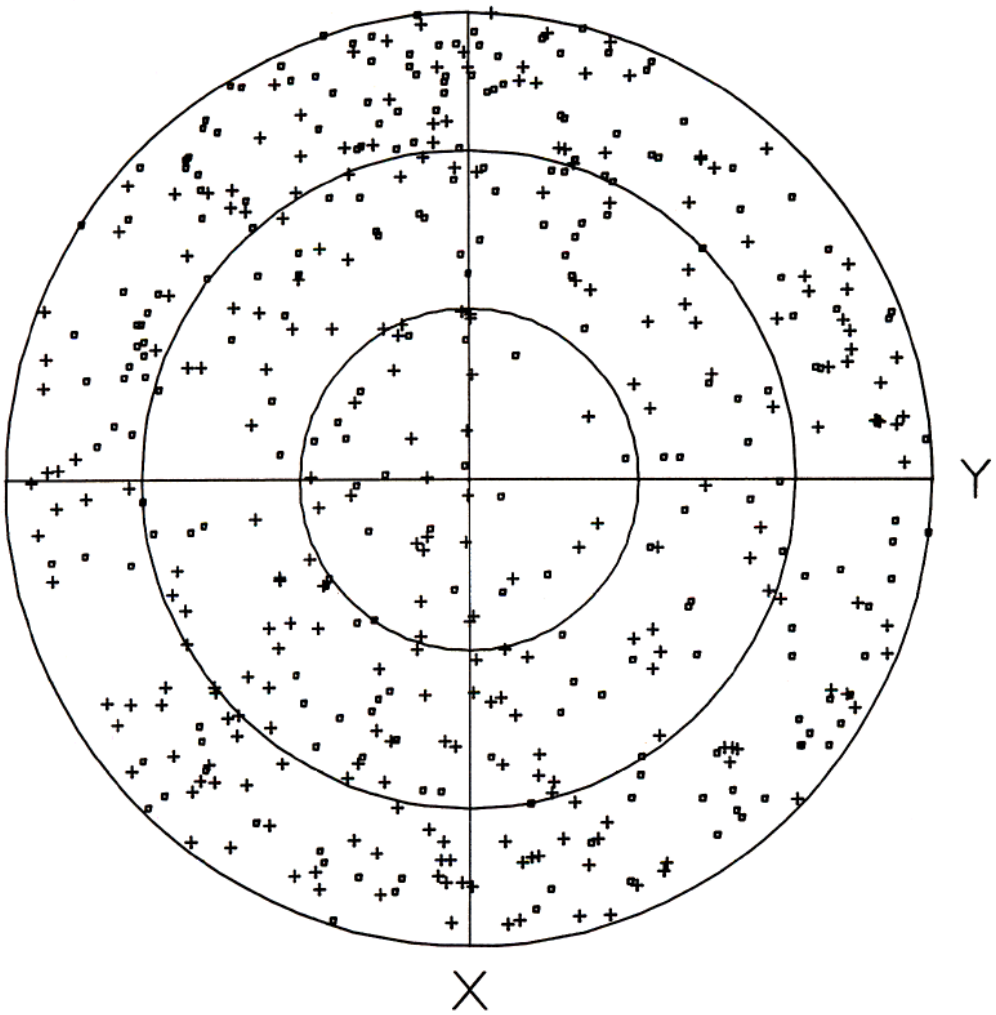

Figure 12. Distribution of preferred directions (n = 475). *A,* 3-D plot. *B,* Equal-area projection plot. See text for explanation.

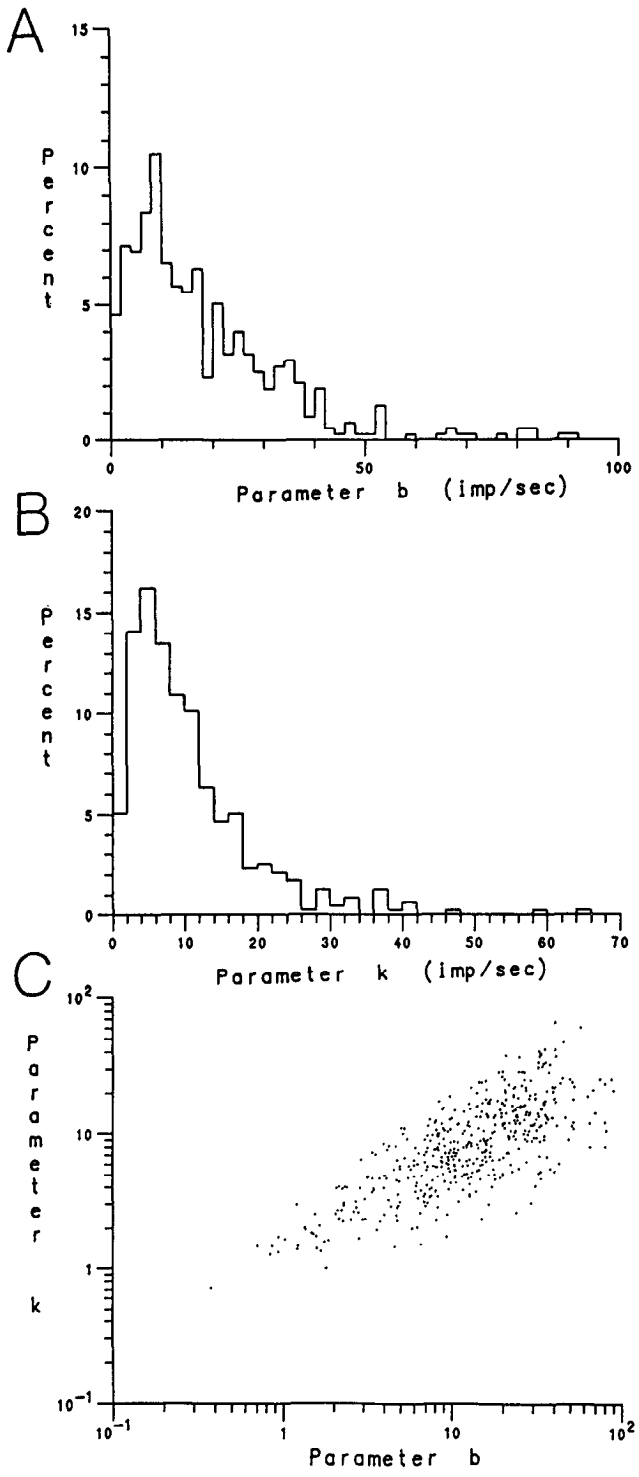

Figure 13. *A*, Distribution of tuning parameter *b*. *B*, Distribution of tuning parameter *k*. *C*, Scatter plot of *k* versus *b*. $n = 475$.

motoneurons seem to be made by corticospinal axons (Phillips and Porter, 1977; Kuypers, 1981). There is little doubt, however, that motor cortical cells do relate to movements about the proximal arm joints and that clear motor effects are observed using intracortical microstimulation (ICMS) (Kwan et al., 1978; Sessle and Wiesendanger, 1982), although at generally higher thresholds than in the hand area (Sessle and Wiesendanger, 1982).

Schmidt et al. (1975) compared the effects on motor cortical

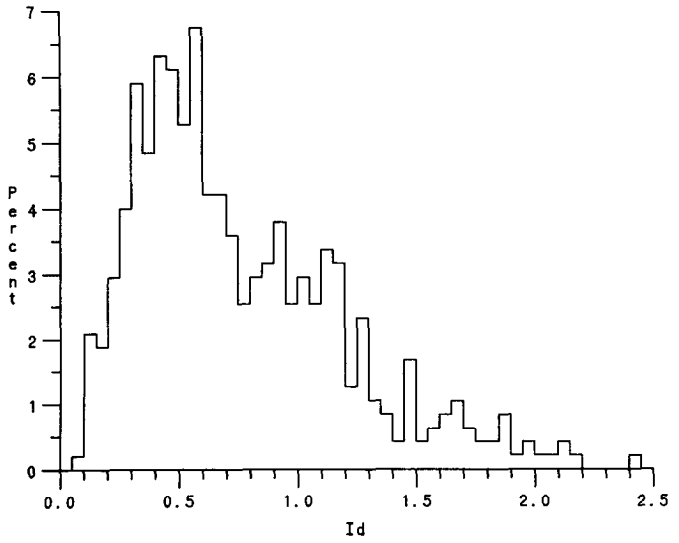

Figure 14. Distribution of index of depth of tuning, I_d ($n = 475$).

cell discharge of force magnitude with those of the direction of movement about the wrist joint: it was found that movement direction was quantitatively more important than force magnitude in characterizing cell activity. Moreover, Thach (1978) observed that changes in activity related to the direction of movement about the wrist joint were independent of the muscle pattern that produced the movement in about a third of the cells studied. Similar changes in cell activity related to the direction of movement independently of the underlying muscular pattern have also been described in primate putamen (Crutcher and DeLong, 1984) and globus pallidus (Mitchell et al., 1987).

Motor cortical activity during reaching

Porter and McLewis (1975) described the activity of cells in the motor cortex during unconstrained reaching in behaving mon-

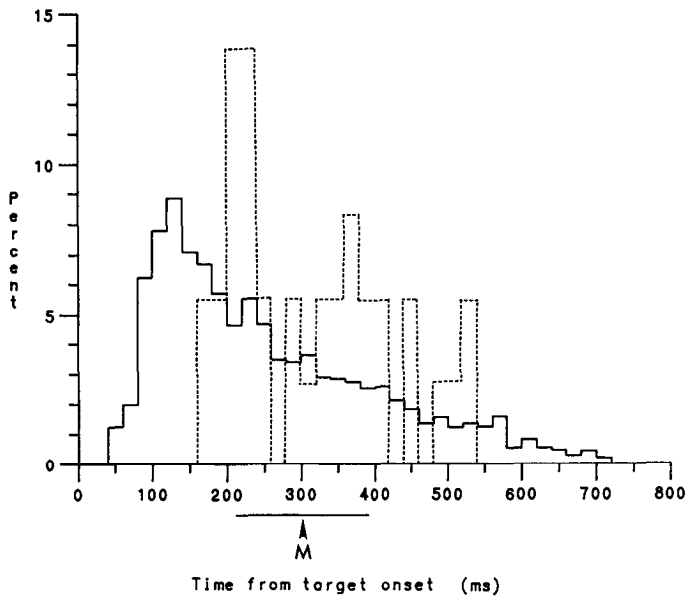

Figure 15. *Solid line*, Distribution of latencies of increases in discharge rate as the first change in cell activity following the target onset (see text). *M*, average (±1 SD) onset of movement. *Dotted line*, Distribution of latencies of increases in EMG activity as the first change (see text).

keys. They found that different cells became active shortly before each of 3 phases of a task that included reaching, grasping, and finally pulling a lever to get a reward. The question of sequential activation of motor cortical cells during reaching was further investigated by Murphy et al. (1985), who recorded the discharge of single cells during reaching to a target positioned in front of the monkey. This movement involved a sequential activation of proximal and distal muscles with the muscles of the shoulder, upper arm, forearm, and hand being activated in sequence. Single cells were functionally identified according to the joint(s) about which motion was produced using ICMS. It was found that the latency of activation of single cells in the task was in accordance with their functional identification. Thus, cells identified by ICMS or passive sensory examination as related to movements about the shoulder or elbow were activated at the earliest time, at about 60 msec after the onset of stimulus (Murphy et al., 1985, Fig. 3); in contrast, cells related to wrist or finger movements were activated last.

A detailed examination of the activity of cells related to motion about the proximal joints of the elbow and shoulder during reaching was carried out by Murphy et al. (1982). ICMS at the site of single-cell recording produced, for every cell studied, a simple joint rotation. There were 3 main findings of this study. First, no simple relation was observed between single-cell activity and the EMG, even when the muscle from which the EMG was recorded was activated by ICMS. Second, single cells related to motion about the shoulder or elbow joints behaved similarly in the task, although the motions produced about these joints could be quite different. And third, the discharge of shoulder-related cells varied systematically with the movement trajectory.

The results of the studies summarized above suggest that the relations between the activity of single motor cortical cells and unconstrained reaching movements are often complex and that changes in cell activity cannot be easily predicted from the effects of ICMS in the region of recording. However, there is little doubt that these cells do participate in the generation of movement and that they are found in cortical regions from which definite motor effects can be produced by ICMS. The studies by Murphy et al. (1982, 1985) seem to indicate that reference of the motor cortical output to motion about single joints or particular muscles does not provide a good characterization of the changes in cell activity. It is possible that these motor output lines may be selected and engaged during the generation of movement using other principles. We suggest that one such principle is the intended trajectory of the hand in space.

Directional tuning

We took this approach when changes in motor cortical cell activity were analyzed in relation to the *direction of arm movement in space* rather than motion about a particular joint (Georgopoulos et al., 1982). These studies were restricted to neurons associated with arm movements about the proximal joints of the shoulder and/or elbow. Since it is motion about these joints that transports and positions the hand in immediate extrapersonal space, it was hypothesized that inputs to the motor cortex from other brain areas might engage the cell populations in the proximal arm area *in terms of the desired arm trajectory* rather than movement about a particular joint. Movement direction was chosen as the meaningful spatial variable for study in relation to motor cortical cell activity. For that purpose a task was designed in which the direction of movement was varied in 2-D space and the activity of motor cortical cells was analyzed. The relations observed between single-cell activity and the direction of movement were relatively simple: most cells possessed a preferred direction but were broadly tuned. Thus, although a cell discharged at high rates with movements in a particular, preferred direction, it also discharged with movements in other directions but at progressively lower rates. This orderly decrease in cell activity was described by a cosine function. The same result was obtained in the present studies and thus generalizes to unconstrained arm movements in 3-D space.

It is noteworthy that a broad tuning function has been found in other cases in which the variation in discharge rate of CNS neurons of diverse systems has been analyzed in relation to directional variables. For example, such a function has been found to describe the relations between the steady-state frequency of discharge of motor cortical cells and the direction of the X-Y force exerted by the hand under isometric conditions (Kalaska and Hyde, 1985); the relations between the discharge of neurons in the pontine reticular formation and the direction of saccadic eye movements (Henn and Cohen, 1976); the relations between single-cell discharge in the middle temporal visual area (Maunsell and van Essen, 1983) and area 7 of the parietal cortex (Steinmetz, et al., 1987) and the direction of moving visual stimuli; the relations between discharge in vestibular neurons and the direction of head tilt (Schor et al., 1984); and the relations between discharge in spinal interneurons and the direction of body motion relative to the body (Wilson et al., 1984; Suzuki et al., 1985). It should be noted, however, that in other cases relatively sharp tuning has been observed (Hubel and Wiesel, 1977).

The activity of 11% of the cells studied in the present experiments did not differ significantly among different movement directions (see, for example, Fig. 11). The role of these cells remains to be elucidated.

Proximal arm movements and reaching

The behavioral goal of reaching is to transport the hand in immediate extrapersonal space, a goal achieved by varying the angles about the shoulder and elbow joints. A recent advance concerning the spinal mechanisms subserving proximal reaching movements has come from the studies of the propriospinal system in the cat by Lundberg and his colleagues (see Lundberg, 1979, for a review). These workers identified propriospinal neurons at the C3–C4 level that project monosynaptically to motoneurons of proximal muscle pools, and receive, in turn, monosynaptic input from several supraspinal systems, including the corticospinal system. In a series of behavioral studies in which the propriospinal and corticospinal projections were interrupted surgically in various combinations, it was found that disturbances of reaching or grasping movements could be dissociated (Alstermark et al., 1981). Reaching depended on the propriospinal projections to the motoneuronal pools, whereas grasping depended upon the projections of the cortico- and rubrospinal systems on the spinal segments at the level of motoneuronal pools innervating distal muscles, caudal to C3–C4 level. Interruption of the corticospinal system above that level disrupted both reaching and grasping movements. These results suggest that reaching movements could be subserved, at the spinal level, by the propriospinal neuronal system, which can be engaged by the corticospinal and other descending systems. Activation of the propriospinal neurons could result in patterned activation of motoneuronal pools innervating proximal muscles. Thus, it

is conceivable that some aspects of reaching movement could be patterned in the spinal cord, specified by supraspinal systems, and emitted as patterned multimuscle activation.

Motor cortical control of limb musculature

The motor cortex can influence the spinal motor apparatus both directly, through the corticospinal tract, and indirectly, through subcortical descending systems. With respect to the corticospinal tract, motor cortical cells synapse on spinal interneurons but also directly upon motoneurons; however, the direct monosynaptic route seems to be restricted to projections to motoneuronal pools innervating distal muscles (Phillips and Porter, 1977). Anatomically, corticospinal axons that originate from the distal limb areas of the motor cortex terminate within regions of both interneuronal laminae and motor nuclei, but axons originating from the proximal arm area seem to terminate mainly in spinal interneuronal zones, at least in the rhesus monkey (Kuypers, 1981). Thus, motor cortical signals relating to proximal arm movements are conveyed to motoneurons *indirectly* through interneurons, both at the segmental level and via the propriospinal system. This is important to keep in mind, for frequently the motor cortical discharge is assumed to drive the motoneuronal pools directly: although this may be true for pools innervating distal muscles in the primate, it does not seem to be the case for pools innervating proximal muscles and, correspondingly, for signals arising from the arm area of the motor cortex.

It is also clear that motor cortical axons diverge appreciably in their projection to the cord (Shinoda et al., 1979, 1981). Although the density of projections can differ for different spinal segments, it is clear that there is not a one-to-one relationship between a motor cortical cell and a motoneuronal pool. Instead, most motor cortical cells seem to influence several pools with varying synaptic potency. This has been shown physiologically in a series of studies (Fetz and Finocchio, 1975; Fetz and Cheney, 1978, 1980; Cheney and Fetz, 1985; Cheney et al., 1985; Lemon et al., 1986). The technique of spike-triggered averaging of EMG activity was used to detect possible monosynaptic connections between motor cortical cells projecting to the spinal cord and motoneuronal pools innervating muscles acting on the hand. Evidence was found of divergent monosynaptic facilitation from single motor cortical cells to more than one motoneuronal pool. A more detailed investigation of the patterns of connections from motor cortical cells to motoneuronal pools was carried out recently (Cheney and Fetz, 1985; Cheney et al., 1985; Lemon et al., 1986). The same technique was used but was applied both to neuronal impulses and to single stimuli delivered through ICMS. Essentially, the results obtained by both methods were similar in that a variety of patterns of influence of the motor cortex upon groups of muscles was revealed.

Directional tuning and muscle events

In the present task, movements in particular directions were produced by the concomitant activation of several muscles; this, and the evidence summarized in the preceding section, suggests that motor cortical cells might relate to *weighted combinations of muscles.* Assume that a motor cortical cell influences directly or indirectly the motoneuronal pools of several muscles. Assume also that these influences differ from cell to cell, so that different cells relate to different weighted combinations of motoneuronal pools: there will be a large number of cells reflecting these combinations, even if the pools involved are few. This arrangement would provide a rich substrate for the motor cortical control of multidimensional arm movements.

Similar considerations have been advanced recently concerning the control of muscles participating in the generation of isometric torques in different directions about the elbow joint (Buchanan et al., 1986). It was found that individual muscles were active with torques in several directions and that, conversely, the application of torques in a particular direction involved always the combined activity of several muscles. It was postulated that the controlled unit might consist of combinations of muscles and that this control might be mediated through premotor interneurons.

If, indeed, motor cortical cells relate to various weighted combinations of muscles, it is interesting to speculate on the functional meaning of the neuronal directional tuning function. At face value, this function relates the frequency of cell discharge to the direction of movement in space. If this direction is considered an input to the motor cortex, in the series of events that precede the generation of the movement, the hypothesized association of single cells to combinations of muscles could be regarded as part of a mechanism that translates this directional input into graded muscle output implementing that direction of movement in space.

References

Alstermark, B., A. Lundberg, U. Norrsell, and E. Sybirska (1981) Integration in descending motor pathways controlling the forelimb in the cat. 9. Differential behavioral defects after spinal cord lesions interrupting defined pathways from higher centres to motoneurones. Exp. Brain Res. *42:* 299–318.

Armitage, P. (1975) *Sequential Medical Trials,* Wiley, New York.

Buchanan, T. S., D. P. J. Almdale, J. L. Lewis, and W. J. Rymer (1986) Characteristics of synergic relations during isometric contractions of human elbow muscles. J. Neurophysiol. *56:* 1225–1241.

Cheney, P. D., and E. E. Fetz (1980) Functional classes of primate corticomotoneuronal cells and their relation to active force. J. Neurophysiol. *44:* 773–791.

Cheney, P. D., and E. E. Fetz (1985) Comparable patterns of muscle facilitation evoked by individual corticomotoneuronal (CM) cells and by single intracortical microstimuli in primates: Evidence for functional groups of CM cells. J. Neurophysiol. *53:* 786–804.

Cheney, P. D., E. E. Fetz, and S. S. Palmer (1985) Patterns of facilitation and suppression of antagonist forelimb muscles from motor cortex sites in the awake monkey. J. Neurophysiol. *53:* 805–820.

Chubbuck, J. G., and A. P. Georgopoulos (1984) A system for recording limb motion in a three-dimensional space. Soc. Neurosci. Abstr. *10:* 337.

Cochran, W. G., and G. M. Cox (1957) *Experimental Designs,* 2nd ed., Wiley, New York.

Crutcher, M. D., and M. R. DeLong (1984) Single cell studies of the primate putamen. II. Relations to direction of movements and pattern of muscular activity. Exp. Brain Res. *53:* 244–258.

Draper, N. R., and H. Smith (1981) *Applied Regression Analysis,* 2nd ed., Wiley, New York.

Duffy, F. H., and J. L. Burchfiel (1971) Somatosensory system: Organizational hierarchy from single units in monkey area 5. Science *172:* 273–275.

Ellaway, P. H. (1977) An application of cumulative sum technique (cusums) to neurophysiology. J. Physiol. (Lond.) *265:* 1–2P.

Ellaway, P. H. (1978) Cumulative sum technique and its application to the analysis of peristimulus histograms. Electroencephalogr. Clin. Neurophysiol. *45:* 302–304.

Evarts, E. V. (1981) Role of the motor cortex in voluntary movements in primates. In *Handbook of Physiology. The Nervous System II,* pp. 1083–1120, American Physiological Society, Bethesda, MD.

Fetz, E. E., and P. D. Cheney (1978) Muscle fields of primate corticomotoneuronal cells. J. Physiol. (Paris) *74:* 239–245.

Fetz, E. E., and P. D. Cheney (1980) Postspike facilitation of forelimb muscle activity by primate corticomotoneuronal cells. J. Neurophysiol. *44:* 751–772.

Fetz, E. E., and D. V. Finocchio (1975) Correlations between activity of motor cortex cells and arm muscles during operantly conditioned response patterns. Exp. Brain Res. *3*:217–240.

Fromm, C. (1983) Changes of steady state activity in motor cortex consistent with the length-tension relation of the muscle. Pfluegers. Arch. *398:* 318–323.

Georgopoulos, A. P., and J. T. Massey (1985) Static versus dynamic effects in motor cortex and area 5: Comparison during movement time. Behav. Brain Res. *18:* 159–166.

Georgopoulos, A. P., J. F. Kalaska, and J. T. Massey (1981) Spatial trajectories and reaction times of aimed movements: Effects of practice, uncertainty, and change in target location. J. Neurophysiol. *46:* 725–743.

Georgopoulos, A. P., J. F. Kalaska, R. Caminiti, and J. T. Massey (1982) On the relations between the direction of two-dimensional arm movements and cell discharge in primate motor cortex. J. Neurosci. *2:* 1527–1537.

Georgopoulos, A. P., R. Caminiti, J. F. Kalaska, and J. T. Massey (1983) Spatial coding of movement: A hypothesis concerning the coding of movement direction by motor cortical populations. Exp. Brain Res. (Supp.) *7:* 327–336.

Georgopoulos, A. P., J. F. Kalaska, M. D. Crutcher, R. Caminiti, and J. T. Massey (1984) The representation of movement direction in the motor cortex: Single cell and population studies. In *Dynamic Aspects of Neocortical Function,* G. M. Edelman, W. E. Gall, and W. M. Cowan, eds., pp. 501–524, Wiley, New York.

Georgopoulos, A. P., J. F. Kalaska, and R. Caminiti (1985) Relations between two-dimensional arm movements and single cell discharge in motor cortex and area 5: Movement direction versus movement endpoint. Exp. Brain Res. (Suppl.) *10:* 175–183.

Georgopoulos, A. P., A. B. Schwartz, and R. E. Kettner (1986) Neuronal population coding of movement direction. Science *233:* 1416–1419.

Georgopoulos, A. P., R. E. Kettner, and A. B. Schwartz (1988) Primate motor cortex and free arm movements to visual targets in three-dimensional space. II. Coding of the direction of movement by a neuronal population. J. Neurosci. *8:* 2928–2937.

Henn, V., and B. Cohen (1976) Coding of information about rapid eye movements in the pontine reticular formation of alert monkeys. Brain Res. *108:* 307–325.

Hepp-Reymond, M. C., U. R. Wyss, and R. Anner (1978) Neuronal coding of static force in the primate motor cortex. J. Physiol. (Paris) *74:* 287–291.

Howell, A. B., and W. L. Straus (1933) The muscular system. In *The Anatomy of the Rhesus Monkey,* E. G. Hartman and W. L. Straus, eds., pp. 89–175, Hafner, New York.

Hubel, D. H., and T. N. Wiesel (1977) Functional architecture of macaque monkey visual cortex. Proc. R. Soc. London [Biol.] *198:* 1–59.

Humphrey, D. R. (1979) On the cortical control of visually directed reaching: Contributions by nonprecentral motor areas. In *Posture and Movement,* R. E. Talbott and D. R. Humphrey, eds., pp. 51–112, Raven, New York.

Kalaska, J. F., and M. L. Hyde (1985) Area 4 and area 5: Differences between the load-dependent discharge variability of cells during active postural fixation. Exp. Brain Res. *59:* 197–202.

Kalaska, J. F., R. Caminiti, and A. P. Georgopoulos (1983) Cortical mechanisms related to the direction of two-dimensional arm movements: Relations in parietal area 5 and comparison with motor cortex. Exp. Brain Res. *51:* 247–260.

Kalaska, J. F., D. A. D. Cohen, and M. L. Hyde (1985) Differences in the spatial relation between movement direction dependent and load direction-dependent activity changes in primate cortex areas 4 and 5. Soc. Neurosci. Abstr. *11:* 1273.

Kuypers, H. G. J. M. (1981) Anatomy of the descending pathways. In *Handbook of Physiology. The Nervous System II,* pp. 597–666, American Physiological Society, Bethesda, MD.

Kwan, H. C., W. A. MacKay, J. T. Murphy, and Y. C. Wong (1978) Spatial organization of precentral cortex in awake primates. II. Motor outputs. J Neurophysiol. *41:* 1120–1131.

Lemon, R. N., G. W. H. Mantel, and R. B. Muir (1986) Corticospinal facilitation of hand muscles during voluntary movement in the conscious monkey. J. Physiol. (Lond.) *381:* 497–527.

Lundberg, A. (1979) Integration in a propriospinal motor centre controlling the forelimb in the cat. In *Integration in the Nervous System,* H. Asanuma and V. S. Wilson, eds., pp. 47–69, Igaku-Shoin, Tokyo.

Mardia, K. V. (1972) *Statistics of Directional Data,* Academic, New York.

Maunsell, J. H. R., and D. C. van Essen (1983) Functional properties of neurons in middle temporal visual area of the macaque monkey. I. Selectivity for stimulus direction, speed, and orientation. J. Neurophysiol. *49:* 1127–1147.

Mitchell, S. J., R. T. Richardson, F. H. Baker, and M. R. DeLong (1987) The primate globus pallidus: Neuronal activity related to direction of movement. Exp. Brain Res. *68:* 491–505.

Mountcastle, V. B., W. H. Talbot, H. Sakata, and J. Hyvarinen (1969) Cortical neuronal mechanisms in flutter-vibration studied in unanesthetized monkeys. Neuronal periodicity and frequency discrimination. J. Neurophysiol. *32:* 452–484.

Mountcastle, V. B., J. C. Lynch, A. Georgopoulos, H. Sakata, and C. Acuna (1975) Posterior parietal association cortex of the monkey: Command functions for operations within extrapersonal space. J. Neurophysiol. *38:* 871–908.

Murphy, J. T., H. C. Kwan, W. A. MacKay, and Y. C. Wong (1982) Precentral unit activity correlated with angular components of a compound arm movement. Brain Res. *246:* 141–145.

Murphy, J. T., Y. C. Wong, and H. C. Kwan (1985) Sequential activation of neurons in primate motor cortex during unrestrained forelimb movement. J. Neurophysiol. *53:* 435–445.

Phillips, C. G., and R. Porter (1977) *Corticospinal Neurones,* Academic, New York.

Porter, R., and M. McLewis (1975) Relationship of neuronal discharges in the precentral gyrus of monkeys to the performance of arm movements. Brain Res. *98:* 21–36.

Sakata, H., Y. Takaoka, A. Kawarasaki, and H. Shinutani (1973) Somatosensory properties of neurons in the superior parietal cortex (area 5) of the rhesus monkey. Brain Res. *64:* 85–102.

Schmidt, E. M., R. G. Jost, and K. K. Davis (1975) Reexamination of the force relationship of cortical cell discharge patterns with conditioned wrist movements. Brain Res. *83:* 213–223.

Schor, R. H., A. D. Miller, and D. L. Tomko (1984) Responses to head tilt in cat central vestibular neurons. I. Direction of maximum sensitivity. J. Neurophysiol. *51:* 136–146.

Sessle, B. J., and M. Wiesendanger (1982) Structural and functional definition of the motor cortex in the monkey (*Macaca fascicularis*). J. Physiol. (Lond.) *323:* 245–265.

Shinoda, Y., P. Zarzecki, and H. Asanuma (1979) Spinal branching of pyramidal tract neurons in the monkey. Exp. Brain Res. *34:* 59–72.

Shinoda, Y., J. I. Yokota, and T. Futami (1981) Divergent projections of individual corticospinal axons to motoneurons of multiple muscles in the monkey. Neurosci. Lett. *23:* 7–12.

Snedecor, G. W., and W. G. Cochran (1980) *Statistical Methods,* 7th ed., Iowa State University Press, Ames, Iowa.

Steinmetz, M. A., B. C. Motter, C. J. Duffy, and V. B. Mountcastle (1987) Functional properties of parietal visual neurons: Radial organization of directionalities within the visual field. J. Neurosci. *7:* 177–191.

Suzuki, I., S. J. B. Timerick, and V. J. Wilson (1985) Body position with respect to the head or body position in space is coded by lumbar interneurons. J. Neurophysiol. *54:* 123–133.

Thach, W. T. (1978) Correlation of neural discharge with pattern and force of muscular activity, joint position, and direction of intended next movement in motor cortex and cerebellum. J. Neurophysiol. *41:* 654–676.

Watson, G. S. (1956) A test for randomness of directions. Monthly Notices R. Soc. Geophys. (Suppl.) *7:* 160–161.

Watson, G. S. (1983) *Statistics on Spheres,* Wiley, New York

Wilson, V. J., K. Ezure, and S. J. B. Timerick (1984) Tonic neck reflex of the decerebrate cat: Response of spinal interneurons to natural stimulation of neck and vestibular receptors. J. Neurophysiol. *51:* 567–577.

Woolsey, C. N., P. H. Settlage, D. R. Meyer, W. Spencer, P. Hamuy, and A. M. Travis (1950) Patterns of localization in the precentral and "supplementary" motor areas and their relation to the concept of a premotor area. Res. Publ. Assoc. Res. Nerv. Ment. Dis. *30:* 238–264.